JACS
JOURNAL OF THE AMERICAN CHEMICAL SOCIETY
Article
pubs.acs.org/JACS

Fluorescent Probes for Tracking the Transfer of Iron−Sulfur Cluster and Other Metal Cofactors in Biosynthetic Reaction Pathways

James N. Vranish,[†] William K. Russell,[‡] Lusa E. Yu,[‡] Rachael M. Cox,[‡] David H. Russell,[‡] and David P. Barondeau*[,‡]

[†]Department of Biochemistry and Biophysics and [‡]Department of Chemistry, Texas A&M University, College Station, Texas 77842-3012, United States

Supporting Information

ABSTRACT: Iron−sulfur (Fe−S) clusters are protein cofactors that are constructed and delivered to target proteins by elaborate biosynthetic machinery. Mechanistic insights into these processes have been limited by the lack of sensitive probes for tracking Fe−S cluster synthesis and transfer reactions. Here we present fusion protein- and intein-based fluorescent labeling strategies that can probe Fe−S cluster binding. The fluorescence is sensitive to different cluster types ([2Fe−2S] and [4Fe−4S] clusters), ligand environments ([2Fe−2S] clusters on Rieske, ferredoxin (Fdx), and glutaredoxin), and cluster oxidation states. The power of this approach is highlighted with an extreme example in which the kinetics of Fe−S cluster transfer reactions are monitored between two Fdx molecules that have identical Fe−S spectroscopic properties. This exchange reaction between labeled and unlabeled Fdx is catalyzed by dithiothreitol (DTT), a result that was confirmed by mass spectrometry. DTT likely functions in a ligand substitution reaction that generates a [2Fe−2S]−DTT species, which can transfer the cluster to either labeled or unlabeled Fdx. The ability to monitor this challenging cluster exchange reaction indicates that real-time Fe−S cluster incorporation can be tracked for a specific labeled protein in multicomponent assays that include several unlabeled Fe−S binding proteins or other chromophores. Such advanced kinetic experiments are required to untangle the intricate networks of transfer pathways and the factors affecting flux through branch points. High sensitivity and suitability with high-throughput methodology are additional benefits of this approach. We anticipate that this cluster detection methodology will transform the study of Fe−S cluster pathways and potentially other metal cofactor biosynthetic pathways.

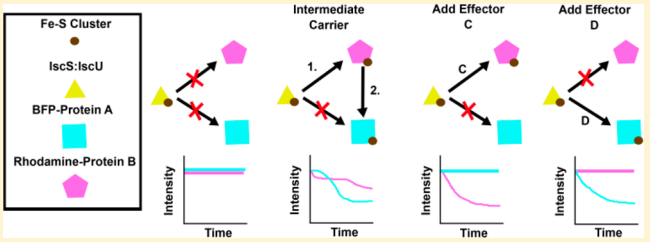

INTRODUCTION

Enzymes require small organic molecules or metal ion cofactors to expand the limited chemical reactivity of amino acids and achieve biological functions. For metal ion cofactors, elaborate biosynthetic and delivery systems have evolved to provide specificity and control indiscriminate reactivity.[1] Delivery systems for some metal cofactors, such as copper and iron−sulfur (Fe−S) clusters, appear to function as a bucket brigade, passing the cofactor from protein to protein until incorporation into the final target.[2] Major challenges for deconvoluting these pathways revolve around establishing which species are kinetically competent intermediates, defining the sequence of transfer reactions, and understanding target specificity. Kinetic experiments are critical to establish whether a transfer reaction is fast enough to be physiologically relevant and to determine which factors affect the flux through transfer branch points. These transfer reactions are often difficult to monitor due to their similar ligand environments and the nearly identical spectroscopic properties of the metal cofactor when it is bound to donor and acceptor proteins. Compromised metallocofactor biosynthesis and trafficking pathways are directly linked to human disease.[3] Thus, the development of strategies to monitor the progress of metal cofactor transfer reactions is highly desirable.

Fe−S clusters are one of the most ubiquitously used and chemically diverse metal cofactors, existing with different ligand environments and stoichiometries, including the commonly found [2Fe−2S] and [4Fe−4S] clusters.[4] Fe−S clusters are best known for their electron transport roles in the respiratory chain and photosynthetic complexes. However, these cofactors also have key roles in substrate binding and activation, initiation of radical chemistry, and sensing small molecules or environmental conditions.[4,5] These clusters are synthesized and delivered by the bacterial NIF, ISC, and SUF systems, and by eukaryotic ISC (in mitochondria), SUF (in chloroplasts), and CIA (in cytosol) systems.[6] The synthesis and delivery of Fe−S clusters is a complex process that appears to involve branched pathways,[7−10] utilize chaperone proteins for some cluster transfer reactions but not others,[11−13] require additional protein factors to convert from [2Fe−2S] clusters to [4Fe−

Received: October 25, 2014
Revised: November 26, 2014
Accepted: December 5, 2014
Published: December 5, 2014

DOI: 10.1021/ja510998s
J. Am. Chem. Soc. 2015, 137, 390−398

4S] clusters,[9,14,15] and necessitate intermediate carrier proteins that provide specificity for selected Fe−S targets.[7,15−17]

Current methodology for monitoring Fe−S cluster assembly and transfer reactions has focused largely on absorption and circular dichroism (CD) spectroscopies.[12,13,16] Absorption spectroscopy is nonideal due to its inability to distinguish clusters bound to donor and acceptor proteins, or even distinguish enzymatic cluster biosynthesis from nonenzymatic Fe−S mineralization or self-assembly chemistry. CD spectroscopy is the best current method to monitor cluster transfer reactions.[12,13,16−20] However, CD spectroscopy has limitations including the requirement for relatively high protein concentrations (10−100 μM), difficulty in detecting some [4Fe−4S] clusters,[21] and interference from other cofactors (such as the PLP in cysteine desulfurase enzymes).[22] Other studies utilize enzyme assays or separation-based techniques that do not allow for facile kinetic analysis and are often limited to reporting the thermodynamics of cluster transfer reactions.[8,23]

Fluorescence spectroscopy has the potential to overcome many of these limitations. Pioneering work using GFP variants, fluorescence resonance energy transfer (FRET), and fusion protein technology led to the development of in vivo metal ion sensors.[24] Similarly, a homoFRET mechanism has been used to monitor the [2Fe−2S] cluster-induced dimerization of glutaredoxin molecules that are fused to GFP variants.[25] Fluorophores associated with small molecules,[26] DNA,[27] or proteins[28] have also been used to report metal ion content or proximity of the metal to the fluorophore. On the basis of these studies, we recognized the potential for a fluorescent labeling approach that would be general for reporting the binding and transfer of Fe−S clusters and would not be limited to Fe−S proteins that oligomerize. Here we show that Fe−S cluster binding can be detected by fluorescence quenching for multiple Fe−S proteins and that this labeling strategy can be used to detect the binding of other metals. We then use this phenomenon to investigate the surprising [2Fe−2S] cluster exchange reaction between labeled and unlabeled ferredoxin.

RESULTS

Generation of Fluorescently-Labeled Fe−S-Containing Proteins. We hypothesized that placing a fluorophore spatially near an Fe−S cluster would create a reporter for cluster binding. Fe−S proteins were labeled with either a blue fluorescent protein (BFP) tag, which is convenient to generate, or a small molecule fluorophore, which minimizes the size of the label and can potentially bring the fluorophore into closer proximity to the cluster. BFP was selected as the fluorescent protein tag as the emission at ∼450 nm had spectral overlap with characteristic absorbance bands (between 400 and 500 nm) for iron−sulfur clusters (Supporting Information, Figure S1), thus increasing the likelihood of energy transfer-based quenching. Sulforhodamine B was selected as a small molecule fluorophore because it is sufficiently different from BFP that both fluorophores may be detected in a combined reaction mixture. The fluorescence emission for rhodamine has a modest spectral overlap with typical Fe−S clusters (Supporting Information, Figure S1) but properties similar to those of Cy3, a fluorophore that has been shown to respond to nearby Fe−S clusters.[27] We adapted a recently developed intein labeling method[29] to specifically label proteins with rhodamine on the C-terminus (Supporting Information, Figure S2), leaving cysteine residues unmodified.

Two BFP fusion and three intein-labeled Fe−S proteins were constructed. The *Escherichia coli* monothiol glutaredoxin (Grx4), which binds a single [2Fe−2S] cluster at a homodimeric interface using a cysteine residue and a glutathione (GSH) molecule from each Grx4 subunit, was labeled with rhodamine ($Grx4_{Rho}$). The *E. coli* ISC ferredoxin, which binds a [2Fe−2S] cluster with four cysteine ligands, was labeled with either a N-terminal blue fluorescent protein (BFP−Fdx) or a C-terminal rhodamine (Fdx_{Rho}) fluorophore. The *E. coli* Rieske protein HcaC, which binds a [2Fe−2S] cluster with two cysteine and two histidine ligands, was labeled with rhodamine ($Rieske_{Rho}$). Finally, the *E. coli* lysine 2,3-aminomutase, which contains a [4Fe−4S] cluster, was labeled as a BFP fusion (BFP−LAM). Near stoichiometric rhodamine incorporation was achieved for intein labeling of Grx4, Fdx, and Rieske (0.76−1.07 fluorophores per protein; Supporting Information, Table S1). These proteins were purified and chemically reconstituted with Fe−S clusters. Size exclusion columns were used to isolate the appropriate oligomeric states for the holo-proteins and remove any aggregated materials or unreacted reagents. Iron and sulfide levels for the proteins (Supporting Information, Table S1) were consistent with efficient reconstitution of appropriate [2Fe−2S] and [4Fe−4S] clusters with the exception of BFP−Fdx. Multiple attempts at reconstituting BFP−Fdx produced protein with less iron (1.5 per protein) and sulfide (1.2 per protein) than expected for a [2Fe−2S] cluster.

Four of the five constructs exhibited substantial quenching upon Fe−S cluster incorporation. Reconstitution of the [2Fe−2S] cluster on $Grx4_{Rho}$ converted the protein from a monomer to a dimer and decreased the fluorescence intensity to ∼48% of that seen in apo-$Grx4_{Rho}$ (Figure 1). Reconstitution of the

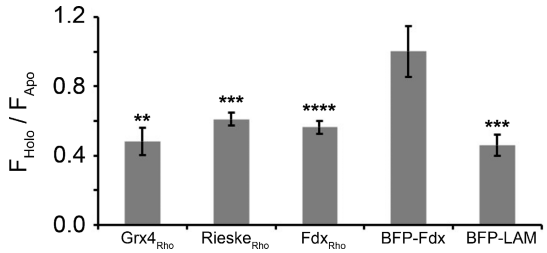

Figure 1. Fluorescence quenching reports Fe−S cluster binding to labeled proteins. The fluorescence intensity was measured for chemically reconstituted proteins and divided by that of the apoprotein. Error bars (SD) are shown for multiple replicates (n = 3). Key: **, $P < 0.01$; ***, $P < 0.001$; ****, $P < 0.0001$.

iron−sulfur clusters for monomeric Fdx_{Rho}, $Rieske_{Rho}$, and BFP−LAM reduced the fluorescence intensity to 56%, 61%, and 46% of the intensity of the apoproteins, respectively (Figure 1). In contrast to Fdx_{Rho}, the BFP−Fdx did not exhibit substantial quenching (Figure 1). Removing the Fe−S cluster from [2Fe−2S]−Fdx_{Rho} recovered the fluorescence intensity (Supporting Information, Figure S3), establishing a correlation between reversible Fe−S cluster binding and fluorescence quenching. Comparing the [2Fe−2S] CD features for Fdx and Fdx_{Rho} revealed that the fluorophore did not significantly perturb the cluster-binding site (Supporting Information, Figure S4). The ability to detect different classes of Fe−S proteins suggests this labeling approach may have broad application in monitoring the cluster content of Fe−S cluster binding proteins.

DOI: 10.1021/ja510998s
J. Am. Chem. Soc. 2015, 137, 390−398

Next, we evaluated the sensitivity of the fluorescent reporter to reagents used in Fe−S assembly assays and to cluster oxidation states. First, we tested if the apoproteins that exhibited cluster-dependent quenching ($Grx4_{Rho}$, $Rieske_{Rho}$, Fdx_{Rho}, and BFP−LAM) were also sensitive to substrates used in Fe−S cluster assembly reactions. In *E. coli*, Fe−S clusters are synthesized by an IscS−IscU complex using L-cysteine, Fe^{2+}, and electrons as substrates.[10] Control Fe−S assembly reactions containing apo-fluorescent target proteins and either ferrous iron or IscS and L-cysteine did not exhibit fluorescence quenching for any of the apo-labeled proteins (Supporting Information, Figure S5). We then focused on the sensitivity of Fdx_{Rho} to individual reagents relevant to Fe−S cluster assembly and transfer reactions. The fluorescence of apo-Fdx_{Rho} was unaffected by addition of Fe^{2+}, NADPH, GSH, DTT, or sulfide (Figure 2). The addition of dithionite slightly quenched the

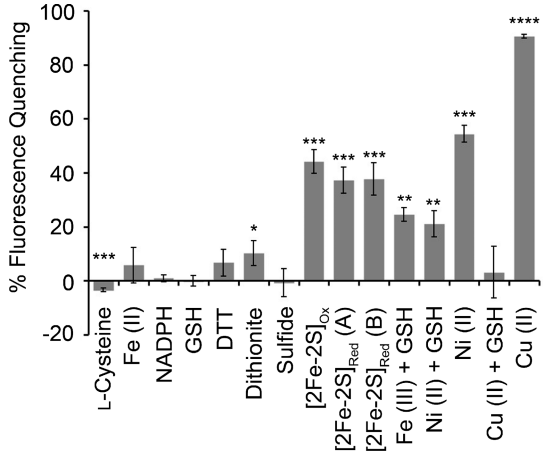

Figure 2. Factors affecting Fdx_{Rho} fluorescence. The fluorescence of apo- or [2Fe−2S]−Fdx_{Rho} was measured immediately after the addition of various reagents and plotted relative to a control containing apo-Fdx_{Rho}. [2Fe−2S] clusters were reconstituted and reduced with dithionite (A) or FldR/NADPH (B). Error bars (SD) are shown for multiple replicates (n = 3). Key: *, $P < 0.05$; **, $P < 0.01$; ***, $P < 0.001$; ****, $P < 0.0001$.

fluorescence (10%), whereas L-cysteine addition slightly enhanced the fluorescence intensity (3%). However, the magnitudes of these changes were small compared to those generated by cluster binding (Figure 2). Moreover, the reporter was sensitive to both oxidized and reduced [2Fe−2S] clusters (Figure 2). Reduction of the cluster by either dithionite or NADPH (with the native Fdx reductant flavodoxin reductase (FldR)) resulted in nearly the same amount of fluorescence quenching (37−38%) as the oxidized cluster. These studies indicate the reporter is sensitive to the binding of either oxidized or reduced Fe−S clusters but largely insensitive to substrates, reagents, and byproducts of Fe−S assembly reactions. Thus, this labeling strategy is a potential new tool for interrogating the kinetics of Fe−S assembly and transfer reactions.

We then tested if the Fdx_{Rho} reporter was sensitive to other metal ion cofactors. Treating apo-Fdx_{Rho} with various metals in the presence of 10 mM GSH revealed significant quenching for Ni^{2+} (21%) and Fe^{3+} (25%) (but not Cu^{2+} (3%)) when compared to the fluorescence of apo-Fdx_{Rho} (Figure 2). Titration of Ni^{2+} into apo-Fdx_{Rho} exhibited binding characteristics (formation of a Ni−Fdx_{Rho} species), an absorbance band at <300 nm, and fluorescence quenching that plateaued at ∼50% of that for apo-Fdx_{Rho} (Supporting Information, Figures S6A,B). Interestingly, the addition of Cu^{2+} in the absence of GSH eliminated the apo-Fdx_{Rho} fluorescence signal (Figures 2 and Supporting Information, S6A). The signal was recovered by subsequent addition of GSH (Supporting Information, Figure S6A), consistent with GSH removing copper from a Cu−Fdx_{Rho} species. Together this suggests binding of the metal to Fdx_{Rho} is critical for quenching. Overall, the sensitivity of the fluorescence to binding of other transition metal species suggests this labeling strategy may also be valuable for investigating additional metal trafficking and biosynthetic pathways.

Facilitation of [2Fe−2S] Cluster Self-Exchange Reactions by DTT. This labeling approach has the potential to advance the enzymology of Fe−S cofactor biosynthesis by allowing the detection of cluster formation on selected proteins in complex reaction mixtures that may contain additional Fe−S proteins and chromophores. The power of this approach is highlighted with an extreme example in which the kinetics of Fe−S cluster transfer reactions are monitored between two Fdx molecules that have identical Fe−S spectroscopic properties. Unlabeled [2Fe−2S]−Fdx and apo-Fdx_{Rho} were reacted in the presence or absence of DTT (Figure 3). In the absence of

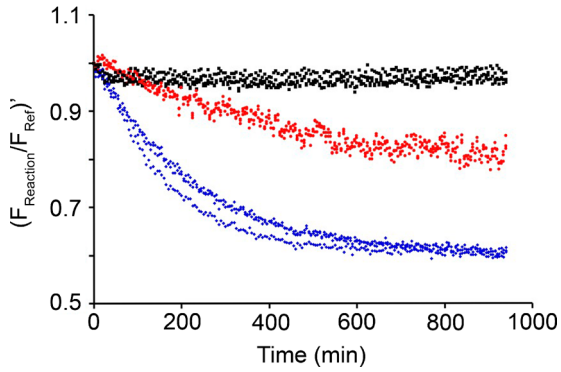

Figure 3. DTT acceleration of cluster transfer from [2Fe−2S]−Fdx to apo-Fdx_{Rho}. [2Fe−2S]−Fdx (20 μM) was incubated with apo-Fdx_{Rho} (1 μM) and 0 (black), 8 (red), or 16 mM (blue) DTT. Three repetitions of each DTT concentration are overlaid. Data were fit as pseudo-first-order reactions in KaleidaGraph (not shown) to determine apparent rates of 0.0013(1) μM cluster min^{-1} (R^2 = 0.955) and 0.004 95(4) μM cluster min^{-1} (R^2 = 0.998) for the 8 and 16 mM DTT reactions, respectively. The minimum fluorescence was assumed to correspond to 1 μM of transferred cluster. The relationship between the apparent rate constants and DTT concentration suggests a second-order reaction with respect to DTT.

DTT, the addition of [2Fe−2S]−Fdx resulted in no significant changes in fluorescence intensity for Fdx_{Rho}. In contrast, addition of both DTT and [2Fe−2S]−Fdx resulted in time-dependent rhodamine quenching with a final intensity (∼60% of initial value) consistent with the formation of a [2Fe−2S]−Fdx_{Rho} species (Figure 1). Increasing the DTT concentration increased the rate of quenching, suggesting a role for DTT in the rate-limiting step for the transfer reaction from [2Fe−2S]−Fdx to apo-Fdx_{Rho} (Figure 3). Substitution of GSH for DTT greatly diminished the quenching rate (Supporting Information, Figure S7). Next, the ratio of [2Fe−2S]−Fdx to apo-Fdx_{Rho} was varied to determine if the extent of fluorescence quenching was consistent with a thermodynamic cluster redistribution and to evaluate the relative cluster binding constants of labeled and

DOI: 10.1021/ja510998s
J. Am. Chem. Soc. 2015, 137, 390−398

unlabeled Fdx (Supporting Information, Figure S8). The final fluorescence intensities (65% for 20:1, 70% for 4:1, and 88% for 1:1) are similar to those calculated (58% for 20:1, 65% for 4:1, and 78% for 1:1; assuming 56% intensity for [2Fe−2S]−Fdx_{Rho} (Figure 1) and identical K_d values). These results are consistent with the cluster on [2Fe−2S]−Fdx being redistributed in a DTT-dependent process between Fdx and Fdx_{Rho} and indicate that these two proteins have similar cluster binding affinities.

A coupled fluorescence and mass spectrometry experiment was used to further interrogate the Fe−S cluster self-exchange reaction on Fdx. A complete reaction containing unlabeled [2Fe−2S]−Fdx, DTT, and apo-Fdx_{Rho} and control reactions lacking either DTT or apo-Fdx_{Rho} were performed. The complete reaction, but not the control lacking DTT, showed time-dependent fluorescence quenching (Supporting Information, Figure S9A). Next, mass spectrometry was used to monitor the loss of cluster from unlabeled [2Fe−2S]−Fdx. The control reactions lacking DTT (Figure 4A) or apo-Fdx_{Rho} (Figure 4B) revealed that the majority of the unlabeled ferredoxin contained a [2Fe−2S] cluster. In contrast, the complete reaction resulted in significant cluster loss from the unlabeled Fdx (Figure 4C). Integrating the signals for all charge species indicated that significantly more apo-Fdx was present in the complete reaction (~50%) than in the control reactions lacking DTT and apo-Fdx_{Rho} (12% and 17%, respectively; Figure 4D). Moreover, the intensity of a peak assigned to [2Fe−2S]−Fdx_{Rho} increased for the complete reaction compared to that of the control reactions (Supporting Information, Figure S9B). These results are consistent with cluster loss from unlabeled [2Fe−2S]−Fdx and DTT-dependent transfer of this species to Fdx_{Rho}. Collectively, fluorescence quenching and mass spectrometry experiments reveal that DTT catalyzes the Fe−S cluster transfer reaction from holo- to apo-Fdx, resulting in the redistribution of [2Fe−2S] clusters. These results also demonstrate that this labeling methodology permits the challenging real time detection of cluster content of a labeled protein in the presence of unlabeled proteins with identical Fe−S spectroscopic properties.

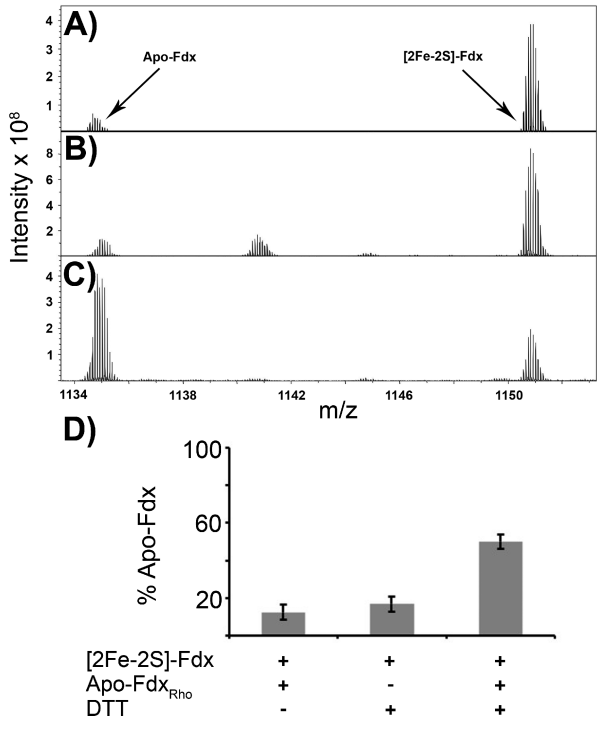

Figure 4. Mass spectrometry revealing DTT-dependent cluster exchange between [2Fe−2S]−Fdx and apo-Fdx_{Rho}. Mass spectra for the +11 charge species of unlabeled Fdx at the conclusion of cluster transfer reactions for samples (A) lacking DTT, (B) lacking apo-Fdx_{Rho}, or (C) a complete reaction with [2Fe−2S]−Fdx (80 μM), apo-Fdx_{Rho} (40 μM), and DTT (20 mM). Deconvolution of m/z peaks identified [2Fe−2S]−Fdx ([M + H] = 12 642.0 Da, expected mass 12 643.7 Da) and apo-Fdx ([M + H] = 12 467.1 Da, expected mass 12 467.9 Da) species. An additional peak in sample B is consistent with apo-Fdx plus two sulfur atoms. (D) Peak intensities for [2Fe−2S]−Fdx and apo-Fdx were integrated for all visible charge states and the percentage of apo-Fdx was plotted for the samples from (A), (B), and (C). The 50% apo-Fdx observed in the presence of DTT and apo-Fdx_{Rho} agrees well with the expected 41% (assuming [2Fe−2S]−Fdx contained 12% apo-Fdx). Error bars represent a standard error of 4%.

Cluster Transfer Acceleration Through DTT-Dependent Ligand Exchange Reaction. The observed Fdx cluster exchange depends on DTT concentration, suggesting that DTT may be functioning in a ligand-substitution reaction to generate a DTT cluster intermediate that can redistribute the cluster between apo-Fdx molecules. However, other possible roles for DTT include (i) preparing the apo-Fdx_{Rho} for cluster transfer by reducing disulfides or chelating adventitiously bound metal ions and (ii) reducing the Fe−S cluster (similar to mitoNEET[30]) resulting in a more labile species. To test the first alternative, Fdx_{Rho} was prereduced with 20 mM DTT for 4 h and then diluted into a cluster transfer reaction containing a final concentration of 8 mM DTT. The additional incubation time with DTT had no effect on the cluster exchange kinetics (Supporting Information, Figure S10), indicating that DTT is not reducing disulfides on Fdx_{Rho} or chelating bound metals. To test the second alternative, we added reagents known to reduce [2Fe−2S]−Fdx and measured the fluorescence quenching of Fdx_{Rho}. Notably, the oxidized and reduced forms of the Fe−S cluster exhibit similar quenching for [2Fe−2S]−Fdx_{Rho} (Figure 2). Substitution of dithionite for DTT resulted in a very slow quenching of fluorescence (Figure 5). Adding dithionite to standard exchange reactions along with DTT resulted in rates almost identical to the rates of the dithionite-substituted reaction lacking DTT (Figure 5). This indicates that dithionite inhibits DTT-mediated cluster

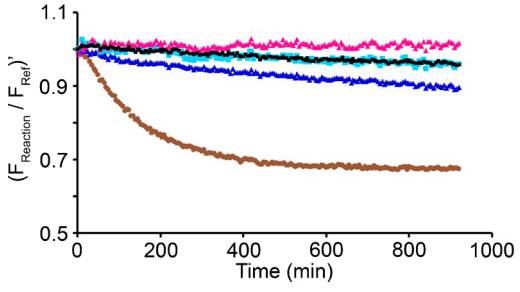

Figure 5. Fdx cluster exchange slowed by reduction. Reactions contained apo-Fdx_{Rho} (0.5 μM) and [2Fe−2S]−Fdx (10 μM) plus (brown) 20 mM DTT, (cyan) 1 mM sodium dithionite, (pink) 50 nM FldR and 100 μM NADPH, (black) 20 mM DTT and 1 mM sodium dithionite, or (dark blue) 20 mM DTT, 50 nM FldR, and 100 μM NADPH. The plotted data is the average of at least three runs for each sample with the maximum error (SD) for any data point being 0.06 $(F_{reaction}/F_{ref})'$.

DOI: 10.1021/ja510998s
J. Am. Chem. Soc. 2015, 137, 390−398

exchange. Substitution of the native ferredoxin electron donation system, FldR and NADPH, for DTT resulted in no cluster exchange (Figure 5). Addition of both DTT and FldR/NADPH resulted in exchange rates that were much slower than reactions with just DTT. Combined, these results suggest that DTT mediates the exchange reaction through a ligand substitution process and that reduced iron−sulfur clusters exchange on a much slower time scale than oxidized clusters. These experiments highlight the advantages of this labeling approach for detecting different types of Fe−S clusters and monitoring the transfer kinetics of these clusters under experimental conditions that would be challenging with other methods.

DISCUSSION

A major challenge for understanding metal trafficking and metal cofactor biosynthesis is the lack of spectroscopic probes for measuring the rates of metal transfer reactions. It is imperative to distinguish between the thermodynamics and the kinetics of in vitro metal transfer reactions. Thermodynamic studies provide much information about whether or not a particular transfer can occur but provide little information about whether or not that transfer is fast enough to be physiologically relevant. Here, two fluorescent labeling strategies were described that successfully report iron−sulfur cluster binding and are well suited to function as kinetic probes for metal transfer reactions. These fluorophore labeling strategies were demonstrated to be effective in reporting the presence of Fe−S clusters with different stoichiometries ([2Fe−2S] and [4Fe−4S] clusters), ligand sets (Grx4, Fdx, and Rieske [2Fe−2S] clusters), and oxidation states ($[2Fe−2S]^{2+}$ and $[2Fe−2S]^{+}$ clusters). Notably, this is in contrast to the difficulties encountered when [4Fe−4S] clusters are observed with CD spectroscopy[21] and when reduced Fe−S clusters are monitored with absorbance spectroscopy. Perhaps the most important advantage of fluorescent labeling over existing methodology is the ability to detect the real-time Fe−S cluster incorporation of a specific labeled protein in the presence of unlabeled Fe−S binding proteins or other chromophores. Additionally, the ability to use different fluorophores with substantially different fluorescent properties permits the simultaneous monitoring of cluster transfer to multiple [2Fe−2S] or [4Fe−4S] binding proteins and the testing of different factors as partitioning determinants for target specificity. This methodology can be used to determine kinetic parameters (k_{cat}, K_i, and K_M values) for a wide variety of cluster transfer reactions, including experiments that evaluate the ability of multiple proteins to compete for a common cluster source. This method represents a vast improvement over other techniques in terms of sensitivity, sample requirements, and range of concentrations that can be used in an assay. An additional benefit is the suitability of these fluorescence probes with high-throughput plate reader methodology. Overall, this labeling methodology will be an excellent complement to CD spectroscopy to monitor metal transfer reactions.

There are multiple strategies for fluorescently labeling metal binding proteins. The first labeling approach, generation of a fusion protein with BFP, is straightforward in that it does not require any subsequent chemistry after protein isolation to incorporate the fluorophore. Fluorescent protein tags can also be beneficial in the solubilization and purification of proteins. However, we observed mixed results using this approach with no observable quenching for BFP−Fdx but strong quenching (54%) upon [4Fe−4S] cluster binding to BFP−LAM. The second approach, intein labeling, allows for the site-specific labeling of any protein on its C-terminus. All three proteins labeled using this intein chemistry exhibited strong cluster-dependent quenching (39−52%). In addition, this labeling approach has many attractive qualities including inexpensive reagents, limited reactivity with amino acid side chains, and high yields.

The fluorescent constructs described here use a variety of different quenching mechanisms. The BFP constructs likely depend on FRET quenching with the cluster acting as an acceptor. FRET is a nonradiative process that depends on the donor−acceptor spectral overlap, varies with donor−acceptor orientation, and can occur over distances of up to 100 Å. In the case of BFP−LAM, the spectral overlap between the [4Fe−4S] cluster absorbance (between 400 and 500 nm) and BFP fluorescent emission (peak at ∼450 nm) and the apparent long distance between the [4Fe−4S] cluster and fluorophore (estimated at >50 Å)[31] are consistent with FRET and not with quenching mechanisms limited to shorter distances. Thus, the quenching for BFP−LAM but not BFP−Fdx may be explained by the greater absorbance of a [4Fe−4S] cluster, the lower cluster content of BFP−Fdx, and/or differences in BFP cluster distances or orientations.

Quenching for the rhodamine constructs may be more complex. In the case of $Grx4_{Rho}$, cluster induced dimerization brings the two rhodamine molecules within the homoFRET distance (R_0 = 55−58 Å).[32] The Fdx_{Rho} and $Rieske_{Rho}$ proteins exhibit quenching similar to that of $Grx4_{Rho}$ upon [2Fe−2S] cluster binding but do not dimerize, ruling out a homoFRET quenching mechanism. Rather, it is likely that these fluorophores are quenched by a combination of FRET (with the cluster acting as an acceptor) and electron transfer. We estimate the distances between the cluster and fluorophore are between 6 and 36 Å on the basis of the crystal structures of Fdx[33] and Rieske.[34] These distances and the spectral overlap between [2Fe−2S] clusters and rhodamine are appropriate for FRET quenching. However, the quenching observed for Ni−Fdx_{Rho}, which has weak spectral overlap between the Ni^{2+} absorbance and rhodamine, suggests a non-FRET mechanism such as electron transfer may also be relevant. Cu^{2+} may quench fluorescence similarly to Ni^{2+} by binding Fdx_{Rho} in the absence (but not presence) of GSH. An alternate explanation for the Cu-based quenching is that GSH affects the ability of Cu to function as a collisional quencher. Additional studies would be required to define the quenching mechanisms for these rhodamine-labeled proteins.

Here we highlight some of the strengths of this labeling methodology by investigating the exchange of [2Fe−2S] clusters between holo-Fdx and apo-Fdx_{Rho}. The [2Fe−2S] clusters on Fdx are resistant to degradation in air and bind with very high affinity.[12,13,16] Despite this thermodynamic stability, the addition of DTT was found to mediate the exchange of [2Fe−2S] clusters between Fdx proteins. The rate dependence on DTT suggests a bimolecular reaction in which both DTT and [2Fe−2S]−Fdx participate in the transition state of the slow step in the reaction. These results support a model in which DTT functions in a ligand substitution reaction to form a [2Fe−2S]−DTT species that redistributes the [2Fe−2S] clusters between Fdx and Fdx_{Rho} (Figure 6). Interestingly, DTT alone was unable to cause a significant loss of cluster from [2Fe−2S]−Fdx (Figure 4D). This suggests that although the cluster is labile in the presence of DTT, the equilibrium lies

DOI: 10.1021/ja510998s
J. Am. Chem. Soc. 2015, 137, 390−398

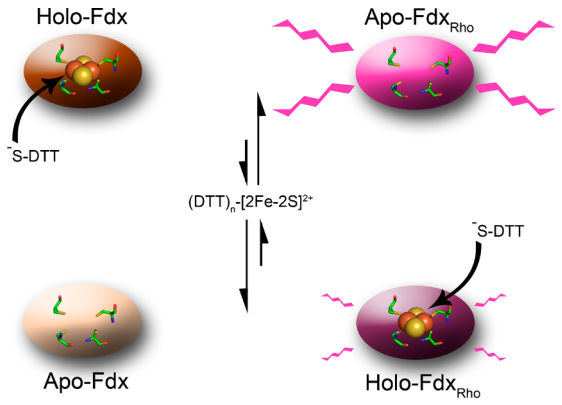

Figure 6. Model of DTT-dependent cluster transfer reaction. DTT initiates a ligand substitution reaction through nucleophilic attack of the $[2Fe-2S]^{2+}$ cluster on Fdx. This forms a DTT−$[2Fe-2S]^{2+}$ cluster species that readily transfers the cluster either back to apo-Fdx or forward to apo-Fdx$_{Rho}$, which results in fluorescence quenching.

toward cluster binding to Fdx (Figure 6). Notably, there is precedent for thiol reagents extruding [2Fe−2S] clusters from proteins.[35]

We further demonstrate that cluster reduction decreases the exchange rate. This is a somewhat surprising result as cluster reduction is often thought, because of the reduced thermodynamic stability of some reduced Fe−S clusters, to trigger transfer reactions in Fe−S cluster biosynthesis. We postulate that the negatively charged DTT molecule is able to bind an oxidized cluster more readily than a reduced cluster, as would be expected on the basis of electrostatic arguments. This lowers the transition state energy for the oxidized [2Fe−2S] cluster more than the reduced cluster, resulting in the observed differences in cluster transfer rate. These results further emphasize the need to examine the kinetics and not just the thermodynamics of metal transfer reactions.

The DTT-dependent acceleration of cluster exchange reactions raises questions about the physiological role of small molecule thiols in cluster transfer. The ligand substitution process described for DTT may be similar to that occurring for physiological cluster transfer reactions. Thiol-containing small molecules such as GSH[36] and trypanothione,[37] which have been proposed as important species in trafficking Fe−S clusters, may mediate in vivo cluster transfer reactions. Alternately, thiol-containing proteins such as monothiol glutaredoxins may mimic DTT and mediate the transfer of Fe−S clusters. It is also possible that the physiological cluster transfer reactions operate through a different mechanism than the ligand substitution exchange reactions mediated by DTT. This is supported by the ability of DTT to greatly enhance Fdx cluster exchange relative to GSH. As the use of DTT is nearly ubiquitous in previous cluster transfer reactions, the transfer rates and conclusions for many of these studies warrant reinvestigation. DTT is likely even more efficient at catalyzing cluster transfer reactions for Fe−S assembly and transfer proteins, which are designed to transiently bind Fe−S clusters, than for the terminal Fe−S acceptor protein Fdx.

In summary, fluorophore labeling strategies were demonstrated to have general application in reporting Fe−S cluster content. An even more dramatic binding signal may be generated by placing the fluorophore near the metal binding site using artificial amino acid technology.[38] The sensitivity of labeled Fe−S acceptor proteins to cluster binding, but insensitivity to Fe^{2+}/sulfide/GSH/NADPH (and low sensitivity to cysteine), along with the ability to monitor a labeled protein in the presence of unlabeled Fe−S proteins, will make these probes transformative new tools for investigating in vitro Fe−S cluster assembly reactions. Furthermore, the ability to detect other metal ions suggests that this labeling approach may also have applications in the in vitro studies of additional metal transfer reactions.

MATERIALS AND METHODS

Protein Preparations. A206K/F223L-GFP was cloned into pET28a between the NheI and BamHI sites. Site-directed mutagenesis was used to add a TEV protease cleavage site to the C-terminal end of the GFP gene (pHis−GFP−TEV). The gene coding for *E. coli* Fdx was amplified by PCR and cloned into pHis−GFP−TEV on the C-terminal side of the TEV site using MEGAWHOP40 cloning (pHis−GFP−TEV−FDX). This vector was transformed into Rosetta (DE3) cells. The cells were grown in LB (BD Biosciences) at 37 °C until the OD_{600} reached 0.5 and then β-D-1-thiogalactopyranoside (IPTG) was added to a concentration of 0.5 mM. The temperature was decreased to 20 °C, and the cells were grown for ~16 h. The cells were lysed by sonication (Branson sonifier 450) in 20 mM Tris, 5 mM imidazole, and 500 mM NaCl at pH 7.5, and the supernatant was loaded on a 5 ml Ni-NTA column (GE Life Sciences). The protein was eluted with a gradient to 500 mM imidazole. The resulting fractions were combined, incubated with TEV protease overnight at room temperature, and dialyzed into 50 mM Tris at pH 7.5. The protein was then loaded on a 27 mL anion exchange column (16 mm × 13.5 cm, POROS HQ 50) and eluted with a gradient to 1 M NaCl. The resulting brown fractions were concentrated and loaded on a 26/60 Sephadex 100 column (GE Life Sciences) equilibrated with 50 mM HEPES and 150 mM KCl at pH 7.2. Fractions containing monomeric protein were concentrated, frozen in liquid nitrogen, and stored at −80 °C.

A pET30 vector containing the *E. coli* FldR gene was a generous gift from Dr. Frank Raushel's laboratory. This vector was transformed into *E. coli* strain BL21 (DE3). Cells were grown at 37 °C until they reached an OD_{600} of 0.6. At that point, the temperature was decreased to 16 °C and protein expression was induced with 0.5 mM IPTG. Cells were harvested 16 h later. Cells were resuspended in 50 mM Tris, 5 mM imidazole, and 250 mM NaCl at pH 7.8 and ruptured by sonication. Soluble material was loaded onto a 5 mL Ni-NTA column (GE Life Sciences) and eluted with a linear gradient to 400 mM imidazole. Yellow fractions were concentrated and dialyzed into 50 mM Tris and 250 mM NaCl at pH 7.8. The protein was loaded onto a 26/60 Sephacryl S300 column (GE Life Sciences) equilibrated with 50 mM HEPES and 250 mM NaCl at pH 7.5. Protein concentration was estimated by using a FAD extinction coefficient of 11 300 M^{-1} cm^{-1} at 450 nm.[41]

BFP (GFP-sol variant[39] with Y66H and H145F substitutions) and a C-terminal tetraglycine linker were cloned into a pET28a vector after the N-terminal His-tag using the MEGAWHOP[40] protocol. *E. coli* ferredoxin (Fdx) and lysine aminomutase (LAM) were amplified from genomic DNA and cloned into the BFP vector on the C-terminal side of the tetraglycine linker. In addition, Fdx, Grx4, and Rieske (HcaC subunit of 3-phenylpropionate dioxygenase) were PCR amplified from *E. coli* genomic DNA and cloned into the NdeI and XhoI sites of pTwin1−His (Jena Bioscience). DNA

DOI: 10.1021/ja510998s
J. Am. Chem. Soc. 2015, 137, 390−398

sequences were confirmed by the Texas A&M Gene Technology Lab.

Five vectors (BFP−Fdx, BFP−LAM, pTwin1−His−Fdx, pTwin1−His−Grx4, and pTwin1−His−Rieske) were separately transformed into Rosetta (DE3) cells and grown in LB medium (BD Biosciences) at 37 °C until the OD_{600} reached 0.5−1.0. The temperature was decreased to 25 °C and protein expression was induced with 0.5 mM IPTG for 16 h. The cells were collected by centrifugation and disrupted by sonication in 20 mM Tris, 5 mM imidazole, and 500 mM NaCl at pH 7.5. The lysate was loaded on a 5 mL Ni-NTA column (GE Life Sciences) and eluted with a gradient to 500 mM imidazole. For the BFP−Fdx and BFP−LAM samples, the proteins were dialyzed and loaded on a 27 mL anion exchange column (POROS HQ 50 μM) with 50 mM Tris at pH 7.5 and eluted with a gradient to 1 M NaCl. The BFP−Fdx and BFP−LAM fractions were concentrated, treated with 1−10 mM DTT, and loaded on a 26/60 Sephadex 300 column (GE Life Sciences) equilibrated with 50 mM Tris and 150 mM NaCl at pH 7.5. For the samples from pTwin vectors, the eluate from the Ni column was mixed with an equal volume of 400 mM Na_2S and 800 mM KH_2PO_4 and the mixture was incubated for 16 h. (***Safety alert:*** Prepare 400 mM Na_2S and 800 mM KH_2PO_4 in a fume hood by slowly adding 1.6 M KH_2PO_4 to a solution of 800 mM Na_2S.) This step resulted in intein cleavage and production of thiocarboxylate species. The samples were dialyzed against a buffer of 50 mM KPO_4 and 100 mM KCl (pH 6.0) in a fume hood and reapplied to the Ni column. The cleaved proteins flowed through the column. The samples were concentrated to ∼1 mM and treated for 16 h with greater than 5 equiv of Lissamine−rhodamine B sulfonyl azide, which was synthesized from sulforhodamine B acid chloride (Sigma-Aldrich) and sodium azide (Sigma-Aldrich) as previously described[29] and stored at −20 °C in DMSO. The Fdx_{Rho}, $Grx4_{Rho}$, and $Rieske_{Rho}$ samples were separately applied to a 1 mL anion column and washed extensively with 50 mM Tris pH 7.5 buffer. Addition of up to 1 M NaCl eluted the pink protein samples from the column. Occasionally, on-column denaturation with 6 M urea and refolding was used to increase the yield. Analysis of the samples by SDS-PAGE and fluorescent gel imaging showed that the protein samples were successfully labeled and that excess fluorophore had been removed. Protein concentrations were determined using a Bradford assay. Rhodamine B was quantitated using the extinction coefficient[42] at 564 nm of 84 000 M^{-1} cm^{-1}. The purified proteins were flash frozen in liquid nitrogen.

Preparation of Apoproteins and Fe−S Cluster Target Proteins. Fe−S clusters were removed from Fdx_{Rho}, BFP−Fdx, $Grx4_{Rho}$, and $Rieske_{Rho}$ by acid precipitation with 10% trichloroacetic acid following incubation with 67 mM D,L-DTT and 67 mM NaOH for at least 5 min at room temperature. Proteins were pelleted and washed five times with 1 mL of metal free water. The proteins were resuspended in 50 mM HEPES and 150 mM KCl at pH 7.2 (buffer A) in an anaerobic glovebox (mBraun, 16 °C, O_2 < 1 ppm). Lysine aminomutase was purified aerobically and did not contain an Fe−S cluster. Thus, the as-isolated protein was treated as apoprotein.

Apoproteins were mixed with 10 mM BME, DTT, or GSH in a buffered solution (typically pH 7.2 for rhodamine-labeling constructs and pH 9.0 for BFP constructs). Ferric chloride and sodium sulfide or ferrous ammonium sulfate and 1 μM IscS, 5 μM IscU, and 1 mM cysteine were used for the cluster reconstitution. The iron and sulfide concentrations were kept below 1 mM. The cluster reconstitution reactions proceeded for 1 h to overnight depending on the particular protein. The reconstituted proteins were desalted with a 5 mL desalting column and applied to a Superdex 200 10/300 size exclusion column (GE Life Sciences). Only protein eluting at the correct size was used for experiments (dimer for Grx4 and monomers for Fdx, Rieske, and LAM). In some cases, a 1 mL monoQ column (Pharmacia Biotech) was used to remove additional iron and sulfide. The ferrozine assay (extinction coefficient of 28 000 M^{-1} cm^{-1} at 562 nm) was used to quantitate iron.[43] For the rhodamine-labeled proteins, the absorbance due to rhodamine was subtracted from the total absorbance (rhodamine plus ferrozine complex) prior to iron quantitation. Sulfide was quantified using a methylene blue assay that included pretreatment of the protein with NaOH and zinc acetate.[44]

Fluorescence Assays. Assays were carried out in a Tecan M200 fluorescent plate reader using top-read fluorescence and bottom-read absorbance measurements. The plate reader is located in an anaerobic glovebox ([oxygen] < 0.5 ppm). Greiner 96 well plates with black sides, clear flat bottoms, and a nonbinding coating were used. Plates were kept in the glovebox overnight before use to allow oxygen dissolved in the plastic to diffuse out. The fluorescence of the BFP proteins was measured with excitation and emission wavelength of 380 and 450 nm, respectively. Rhodamine-labeled proteins were monitored with excitation wavelength of 550 nm and emission wavelengths of 600 nm. Assays were typically monitored for 16 h at 25 °C while covered with low-fluorescent clear tape.

Fluorescence Data Processing. A data processing flowchart is provided as Figure S11, Supporting Information. Raw fluorescence data for the reaction ($F_{measured}$) was corrected for the inner filter effect by recording the absorbance of each sample at the excitation (Abs_{ex}) and emission (Abs_{em}) wavelengths and then calculating the corrected fluorescence ($F_{reaction}$) with the first term of eq 1. For the BFP samples, the plates exhibited significant autofluorescence (F_{auto}) and required subtraction of a second correction term in eq 1.

$$F_{reaction} = F_{measured} \times 10^{(Abs_{ex}+Abs_{em})/2} - F_{auto} \times 10^{(Abs_{ex}+Abs_{em})/2} \quad (1)$$

This second term was obtained from the average fluorescent signals from three wells containing buffer (F_{auto}) and was also corrected for the inner filter effect. A reference sample (F_{ref}) was also used to correct for any photobleaching or adhesion to the plate. F_{ref} was calculated using eq 2 using a second control sample ($F_{control}$) that included the fluorescent protein at the same concentration as the reaction but lacked a reagent necessary to initiate the reaction (holo-ferredoxin in this case). Inner-filter effect and autofluorescence corrections were also applied.

$$F_{ref} = F_{control} \times 10^{(Abs_{ex}+Abs_{em})/2} - F_{auto} \times 10^{(Abs_{ex}+Abs_{em})/2} \quad (2)$$

The fluorescence intensity for the reference sample (F_{ref}) was scaled to be 100% throughout the assay. When the fluorescence signals of the sample and reference wells at time 0 were within error of each other, their fluorescent signals were normalized (by dividing the fluorescence at time t by the fluorescence at time 0) to allow the fluorescence experiment to start at a value of 1. The normalized fluorescence values of the reaction and

DOI: 10.1021/ja510998s
J. Am. Chem. Soc. 2015, 137, 390−398

reference wells were then divided to generate the final $(F_{reaction}/F_{ref})'$ value in eq 3.

$$\left(\frac{F_{reaction}}{F_{ref}}\right)'_t = \left(\frac{F_{reaction,t}}{F_{reaction,t=0}}\right)\Big/\left(\frac{F_{ref,t}}{F_{ref,t=0}}\right) \quad (3)$$

Fe−S Cluster Transfer and Control Reactions. Control quenching reactions included 0.5−5 μM Fdx_{Rho} (either holo- or apo-) in buffer A and were performed at 25 °C. Some reactions included 10 mM GSH at pH 7.2. Reagents tested include L-cysteine (1 mM), ferrous ammonium sulfate (100 μM), NADPH (1 mM), GSH (10 mM), D,L-DTT (20 mM), sodium dithionite (1 mM), sodium sulfide (1 mM), FldR (100 nM) with NADPH (1 mM), ferric chloride (100 μM), nickel(II) chloride (100 μM), and copper(II) sulfate (100 μM). The fluorescence was collected immediately and compared to that of a sample lacking the additives. In separate kinetic control experiments, 5 μM Fdx_{Rho} was incubated either with ferrous ammonium sulfate (100 μM) and GSH (10 mM) or with IscS (5 μM), cysteine (100 μM), and GSH (10 mM) at 25 °C in a solution of buffer A with 10 mM GSH. The fluorescence was collected upon iron or cysteine addition and compared to that of a sample that lacked iron or both IscS and cysteine.

For cluster transfer reactions, apo-Fdx_{Rho} was diluted into a solution of buffer A, typically to a concentration of 5 μM. Reducing agents DTT, GSH, sodium dithionite, or FldR/NADPH were added to the reaction. The reaction was initiated by the addition of holo-Fdx. The samples were mixed by pipetting, and the plate was covered with low-fluorescent plastic tape. The temperature of the plate reader was maintained at 25 °C throughout the assay. Every 5 min, the fluorescence was measured (excitation, 550 nm; emission, 600 nm) along with absorbance at the excitation and emission wavelengths, and the sample was shaken further to prevent localized photobleaching. The reaction was typically allowed to proceed for ∼16 h.

Mass Spectrometry. Complete Fdx cluster transfer assays that included 80 μM [2Fe−2S]−Fdx, 40 μM Fdx_{Rho}, and 20 mM D,L-DTT in buffer A were allowed to proceed overnight. Control reactions lacked Fdx_{Rho} or DTT. Aliquots of 50 μL from the reactions were desalted into 10 mM ammonium acetate using Bio-Rad Microspin 6 columns, diluted 1:10 into 10% acetonitrile, and analyzed by direct infusion into a Bruker 9.4 T FT-ICR-MS. The source voltage was 4000 V, and the mass window was 130−2700 m/z with a transient length of 1.9 s. The data from 40 spectra were averaged. Raw data were deconvoluted using Bruker software.

■ ASSOCIATED CONTENT

Supporting Information

A table showing Fe, sulfide, and fluorophore content of reconstituted proteins and additional figures showing spectral overlap of chromophores, the intein labeling approach, reversibility of quenching, additional quenching controls, stoichiometric quenching behavior, mass spectra of [2Fe−2S]−Fdx_{Rho} following cluster transfer, Fe−S cluster transfer reactions containing GSH or prereduced Fdx_{Rho}, and details of fluorescence data processing are provided free of charge via the Internet at http://pubs.acs.org

■ AUTHOR INFORMATION

Corresponding Author

barondeau@tamu.edu

Funding

This work was supported in part by Texas A & M University and by grants A-1647 from the Robert A. Welch foundation (DPB) and GM096100 from the National Institute of Health (DPB), and a grant from the U.S. Department of Energy (DHR) Division of Chemical Sciences (BES DE-FG02-04ER15520).

Notes

The authors declare no competing financial interest.

■ ACKNOWLEDGMENTS

We are indebted to Dr. Tadhg Begley for advice concerning fluorescent labeling strategies. We thank Chris Putnam and members of our research group (D. J. Martin, Hyeran Choi, Nick Fox, Robert Hoyuela, and Seth Cory) for helpful discussions, Hyeran Choi and Frank Raushel for the gift of FldR, and Michaella Levy for preliminary intein labeling studies.

■ ABBREVIATIONS

Fdx, ferredoxin; Grx, glutaredoxin; LAM, lysine 2,3-aminomutase; HcaC, 3-phenylpropionate dioxygenase ferredoxin subunit; GFP, green fluorescent protein; BFP, blue fluorescent protein; DTT, dithiolthreitol; GSH, reduced glutathione; CD, circular dichroism; PLP, pyridoxal phosphate; FRET, fluorescence resonance energy transfer; Rho, sulforhodamine-B; FldR, ferredoxin/flavodoxin reductase; NADPH, reduced nicotinamide adenine dinucleotide phosphate; FT-ICR-MS, Fourier transform inductively coupled resonance mass spectrometry; IPTG, β-D-1-thiogalactopyranoside

■ REFERENCES

(1) Ba, L. A.; Doering, M.; Burkholz, T.; Jacob, C. *Metallomics* **2009**, *1*, 292.
(2) (a) Nevitt, T.; Ohrvik, H.; Thiele, D. J. *Biochim. Biophys. Acta* **2012**, *1823*, 1580. (b) Lill, R.; Hoffmann, B.; Molik, S.; Pierik, A. J.; Rietzschel, N.; Stehling, O.; Uzarska, M. A.; Webert, H.; Wilbrecht, C.; Muhlenhoff, U. *Biochim. Biophys. Acta* **2012**, *1823*, 1491.
(3) (a) Rouault, T. A.; Tong, W.-H. *Trends Genet.* **2008**, *24*, 398. (b) Kaler, S. G. *Handb. Clin. Neurol.* **2013**, *113*, 1745. (c) Sheftel, A.; Stehling, O.; Lill, R. *Trends Endocrinol. Metab.* **2010**, *21*, 302.
(4) Johnson, D. C.; Dean, D. R.; Smith, A. D.; Johnson, M. *Annu. Rev. Biochem.* **2005**, *74*, 247.
(5) Py, B.; Barras, F. *Nat. Rev. Microbiol.* **2010**, *8*, 436.
(6) (a) Takahashi, Y.; Tokumoto, U. *J. Biol. Chem.* **2002**, *277*, 28380. (b) Jacobson, M. R.; Brigle, K. E.; Bennett, L. T.; Setterquist, R. A.; Wilson, M. S.; Cash, V. L.; Beynon, J.; Newton, W. E.; Dean, D. R. *J. Bacteriol.* **1989**, *171*, 1017. (c) Zheng, L.; Cash, V. L.; Flint, D. H.; Dean, D. R. *J. Biol. Chem.* **1998**, *273*, 13264. (d) Lill, R.; Mühlenhoff, U. *Annu. Rev. Biochem.* **2008**, *77*, 669.
(7) Py, B.; Gerez, C.; Angelini, S.; Planel, R.; Vinella, D.; Loiseau, L.; Talla, E.; Brochier-Armanet, C.; Garcia-Serres, R.; Latour, J.-M.; Ollagnier de Choudens, S.; Fontecave, M.; Barras, F. *Mol. Microbiol.* **2012**, *86*, 155.
(8) Wollenberg, M.; Berndt, C.; Bill, E.; Schwenn, J. D.; Seidler, A. *Eur. J. Biochem.* **2003**, *270*, 1662.
(9) (a) Mühlenhoff, U.; Richter, N.; Pines, O.; Pierik, A. J.; Lill, R. *J. Biol. Chem.* **2011**, *286*, 41205. (b) Krebs, C.; Agar, J.; Smith, A. D.; Frazzon, J.; Dean, D. R.; Huynh, B. H.; Johnson, M. *Biochemistry* **2001**, *40*, 14069.
(10) Agar, J.; Krebs, C.; Frazzon, J.; Huynh, B. H.; Dean, D. R.; Johnson, M. *Biochemistry* **2000**, *39*, 7856.
(11) Maio, N.; Singh, A.; Uhrigshardt, H.; Saxena, N.; Tong, W.-H.; Rouault, T. A. *Cell Metab.* **2014**, *19*, 445.
(12) Chandramouli, K.; Johnson, M. *Biochemistry* **2006**, *45*, 11087.

DOI: 10.1021/ja510998s
J. Am. Chem. Soc. 2015, 137, 390−398

(13) Bonomi, F.; Iametti, S.; Morleo, A.; Ta, D. T.; Vickery, L. E. *Biochemistry* **2011**, *50*, 9641.
(14) (a) Krebs, C.; Agar, J.; Smith, A. D.; Frazzon, J.; Dean, D. R.; Huynh, B. H.; Johnson, M. *Biochemistry* **2001**, *40*, 14069. (b) Tan, G.; Lu, J.; Bitoun, J.; Huang, H.; Ding, H. *Biochem. J.* **2009**, *420*, 463.
(15) Tong, W.-H.; Jameson, G. N. L.; Huynh, B. H.; Rouault, T. A. *Proc. Natl. Acad. Sci. U. S. A.* **2003**, *100*, 9762.
(16) Shakamuri, P.; Zhang, B.; Johnson, M. K. *J. Am. Chem. Soc.* **2012**, *134*, 15213.
(17) (a) Bandyopadhyay, S.; Naik, S.; O'Carroll, I.; Huynh, B. H.; Dean, D. R.; Johnson, M.; Dos Santos, P. *J. Biol. Chem.* **2008**, *283*, 14092. (b) Gupta, V.; Sendra, M.; Naik, S. G.; Chahal, H. K.; Huynh, B. H.; Outten, F. W.; Fontecave, M.; Ollagnier de Choudens, S. *J. Am. Chem. Soc.* **2009**, *131*, 6149. (c) Sheftel, A. D.; Stehling, O.; Pierik, A. J.; Netz, D. J.; Kerscher, S.; Elsasser, H. P.; Wittig, I.; Balk, J.; Brandt, U.; Lill, R. *Mol. Cell. Biol.* **2009**, *29*, 6059.
(18) Mapolelo, D. T.; Zhang, B.; Randeniya, S.; Albetel, A.-N.; Li, H.; Couturier, J.; Outten, C. E.; Rouhier, N.; Johnson, M. K. *Dalton Trans.* **2013**, *42*, 3107.
(19) (a) Gao, H. Y.; Subramanian, S.; Couturier, J.; Naik, S. G.; Kim, S. K.; Leustek, T.; Knaff, D. B.; Wu, H. C.; Vignols, F.; Huynh, B. H.; Rouhier, N.; Johnson, M. K. *Biochemistry* **2013**, *52*, 6633. (b) Mapolelo, D. T.; Zhang, B.; Naik, S. G.; Huynh, B. H.; Johnson, M. K. *Biochemistry* **2012**, *51*, 8056.
(20) Bonomi, F.; Iametti, S.; Morleo, A.; Ta, D.; Vickery, L. *Biochemistry* **2008**, *47*, 12795.
(21) Ryle, M. J.; Lanzilotta, W. N.; Seefeldt, L. C.; Scarrow, R. C.; Jensen, G. M. *J. Biol. Chem.* **1996**, *271*, 1551.
(22) Drsata, J.; Bousova, I.; Malon, P. *J. Pharm. Biomed. Anal.* **2005**, *37*, 1173.
(23) (a) Unciuleac, M.-C.; Chandramouli, K.; Naik, S.; Mayer, S.; Huynh, B. H.; Johnson, M.; Dean, D. R. *Biochemistry* **2007**, *46*, 6812. (b) Qi, W.; Cowan, J. A. *Chem. Commun. (Cambridge, U. K.)* **2011**, *47*, 4989.
(24) Miyawaki, A.; Llopis, J.; Heim, R.; McCaffery, J. M.; Adams, J. A.; Ikura, M.; Tsien, R. Y. *Nature* **1997**, *388*, 882.
(25) Hoff, K. G.; Goodlitt, R.; Li, R.; Smolke, C. D.; Silberg, J. J. *ChemBioChem* **2009**, *10*, 667.
(26) Domaille, D. W.; Que, E. L.; Chang, C. J. *Nat. Chem. Biol.* **2008**, *4*, 168.
(27) Honda, M.; Park, J.; Pugh, R. A.; Ha, T.; Spies, M. *Mol. Cell* **2009**, *35*, 694.
(28) Balint, E. E.; Petres, J.; Szabo, M.; Orban, C. K.; Szilagyi, L.; Abraham, B. *J. Fluoresc.* **2013**, *23*, 273.
(29) Krishnamoorthy, K.; Begley, T. P. *J. Am. Chem. Soc.* **2010**, *132*, 11608.
(30) Landry, A. P.; Ding, H. *J. Biol. Chem.* **2014**, *289*, 4307.
(31) Lepore, B. W.; Ruzicka, F. J.; Frey, P. A.; Ringe, D. *Proc. Natl. Acad. Sci. U. S. A.* **2005**, *102*, 13819.
(32) (a) Iwema, T.; Picciocchi, A.; Traore, D. A.; Ferrer, J. L.; Chauvat, F.; Jacquamet, L. *Biochemistry* **2009**, *48*, 6041. (b) MacDonald, R. I. *J. Biol. Chem.* **1990**, *265*, 13533.
(33) Kakuta, Y.; Horio, T.; Takahashi, Y.; Fukuyama, K. *Biochemistry* **2001**, *40*, 11007.
(34) Senda, M.; Kishigami, S.; Kimura, S.; Fukuda, M.; Ishida, T.; Senda, T. *J. Mol. Biol.* **2007**, *373*, 382.
(35) Que, L.; Holm, R. H.; Mortenson, L. E. *J. Am. Chem. Soc.* **1975**, *97*, 463.
(36) Qi, W.; Li, J.; Chain, C. Y.; Pasquevich, G. A.; Pasquevich, A. F.; Cowan, J. A. *J. Am. Chem. Soc.* **2012**, *134*, 10745.
(37) Comini, M. A.; Krauth-Siegel, R. L.; Bellanda, M. *Antioxid. Redox Signaling* **2012**, *16*, 636.
(38) Kurra, Y.; Odoi, K. A.; Lee, Y. J.; Yang, Y.; Lu, T.; Wheeler, S. E.; Torres-Kolbus, J.; Deiters, A.; Liu, W. R. *Bioconjugate Chem.* **2014**, *25*, 1730.
(39) Barondeau, D. P.; Putnam, C. D.; Kassmann, C. J.; Tainer, J. A.; Getzoff, E. D. *Proc. Natl. Acad. Sci. U. S. A.* **2003**, *100*, 12111.
(40) Miyazaki, K. *Methods Enzymol.* **2011**, *498*, 399.
(41) Koziol, J. *Methods Enzymol.* **1971**, *18*, 253.
(42) Haugland, R. *Handbook of Fluorescent Probes and Research Chemicals*, 6th ed.; Molecular Probes: Eugene, OR, 1996.
(43) Stookey, L. L. *Anal. Chem.* **1970**, *42*, 779.
(44) Suhara, K.; Takemori, S.; Katagiri, M.; Wada, K.; Kobayashi, H. *Anal. Biochem.* **1975**, *68*, 632.

DOI: 10.1021/ja510998s
J. Am. Chem. Soc. 2015, 137, 390−398